

Punching shear capacity of bridge decks regarding compressive membrane action

Sana Amir, Cor van der Veen, Joost Walraven

Department Design and Construction, Structural and Building Engineering, Concrete Structures, Faculty of Civil Engineering and Geosciences, Delft University of Technology, the Netherlands

Ane de Boer

Ministry of Infrastructure and the Environment (Rijkswaterstaat), the Netherlands

In the Netherlands, there are a large number of transversely prestressed concrete bridge decks that have been built in the 60's and 70's of the last century and are found to be shear-critical when assessed using the recently implemented EN 1992-1-1:2005 (CEN 2005). To check the safety of such bridges against the wheel print of the Eurocode Load Model 1, laboratory tests on a 1:2 scale model of a prototype bridge, consisting of a thin, transversely prestressed concrete deck slab cast *in situ* between the flanges of long prestressed concrete girders were carried out. The same bridge was modelled with a finite element program and several nonlinear analyses were carried out to calculate the bearing (punching shear) capacity. The theoretical analysis of the model bridge deck demonstrated that the ultimate load carrying capacity as found from the experiments and the finite element analysis was much higher than predicted by the governing codes. A possible explanation to this anomaly could be the occurrence of "Compressive Membrane Action" (CMA) in the deck slab. A combination of numerical and theoretical approach was developed to incorporate CMA in the Model Code 2010 (*fib* 2012) punching shear provisions for prestressed slabs to determine the ultimate bearing capacity. Results showed an adequate safety margin against the Eurocode design wheel load leading to the conclusion that the existing transversely prestressed concrete bridge decks (about 70 bridges) still have sufficient residual bearing (punching shear) capacity and considerable savings in cost can be made if compressive membrane action is considered in the analysis.

Keywords: Concrete, compressive membrane action, deck slab, prestressing, punching shear

1 Introduction

1.1 Background

One of the major questions that structural engineers all over the world are dealing with is the safety of the existing structures. In the Netherlands, there are around 70 bridges consisting of transversely prestressed deck slabs that have been built in the last century and need to be investigated for their remaining lifetime capacity, if any, against the modern traffic loads. The shear capacity as prescribed by the codes in the recently implemented EN 1992-1-1:2005 (CEN 2005) is more conservative than in the former Dutch code NEN 6720 (1995). As a result, many existing bridges are found to be critical in shear when assessed using the Eurocode. It is therefore important to check if such bridges can still be used for a few more decades, provided they are safe and reliable enough against the modern traffic loads. Therefore, a prototype bridge was selected and experimental, numerical and theoretical approaches were used to investigate its safety against the wheel print of the Eurocode Load Model 1. Laboratory tests on a 1:2 scale model of the bridge, consisting of a thin, transversely prestressed concrete deck slab cast in-situ between the flanges of long prestressed concrete girders, showed punching shear failure of the deck slab with a positive influence of the transverse prestressing level on the load carrying capacity. As part of the numerical investigation, a 3D solid, 1:2 scale model of the real bridge, similar to the experimental model, was developed in the finite element software TNO DIANA 9.4.4 and several nonlinear analyses were carried out to calculate the bearing (punching shear) capacity. Furthermore, a theoretical analysis of the model bridge deck was carried out and it was demonstrated that the ultimate load carrying capacity as found from the experiments and the finite element analysis was much higher than predicted by the governing codes. It was found that the transverse prestressing along with Compressive Membrane Action (CMA) enhanced the bearing capacity of the laterally restrained deck slab. This paper gives an overview of the experimental, numerical and the theoretical research carried out on the model bridge deck, outlines the approach used to incorporate compressive membrane action in the punching shear provisions of the Model Code 2010 (fib 2012) and then investigates the structural safety and reliability of the 1:2 scaled model against the (scaled down) traffic loads. The scope of this paper is limited to the ultimate bearing (punching shear) capacity of the model bridge deck only. Detailed results are described elsewhere (Amir 2014, Amir et al. 2014a and Amir et al. 2014b).

1.2 Compressive membrane action

According to traditional methods of bridge design the flexural capacity was mostly the dominating criterion. Only later on it was discovered that under concentrated wheel loads, the punching shear capacity of the laterally restrained deck slabs is mostly governing over the flexural capacity. This drew attention to a mechanism that was mostly ignored, denoted as compressive membrane action (CMA, Bachelor, 1990). This mechanism can be described as follows: when a load is applied on a laterally restrained slab, its edges tend to move outside and the boundary elements produce a compressive membrane force in the plane of the slab enhancing the bearing capacity in both flexure and punching shear.

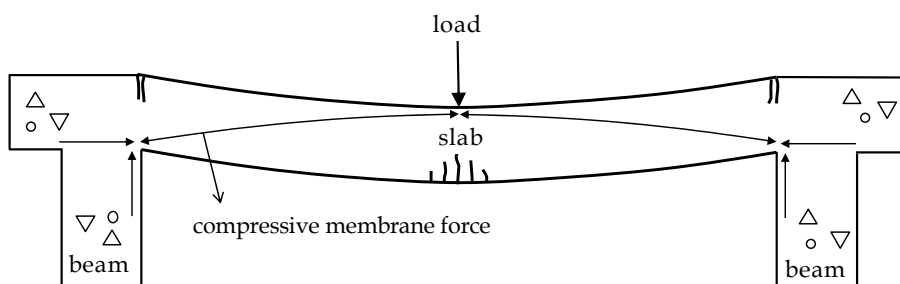


Figure 1. Compressive membrane action in a reinforced concrete bridge deck slab (adapted from Hon et al. 2005)

Up to now, codes like Eurocode 2 (2005) and ACI 318-11 (2011) do not consider CMA in their capacity formulae. However, there are some codes that do consider CMA for reinforced concrete only, like CSA: CHBDC (2006), the Transit New Zealand (2003) Code and UK HA, BD81/02 (2002). This has been possible because CMA has been studied in detail for reinforced concrete deck slabs. Although only limited research was done on prestressed slabs, the expectation was that that CMA will also occur in such slabs. As a result the in-plane forces arising from the combined action of prestressing and compressive membrane forces might increase the bearing capacity to such an extent that there will be no problems with serviceability and structural safety in spite of the low thickness of the slabs.

2 Experimental analysis

2.1 *Real bridge*

In a typical “approach” bridge, the deck slab is quite slender (200 mm thick) and is cast in-situ between the flanges of precast, prestressed concrete girders (3000 mm high and spaced at 3600 mm c/c). The joints between the deck slab and girder flange are indented to generate sufficient shear capacity. The regular reinforcement ratio of the deck slab is quite low as prestressing reinforcement in the transverse direction is present. The prestressing tendons in the slab are placed in the transverse direction at an average spacing of around 650 mm c/c. In some places this spacing is 800 mm c/c. Transversely prestressed end transverse beams are present at the supports, along with diaphragms at 1/3 and 2/3 of the 50 m span. The bridge decks have been cast with normal strength concrete; however, currently the concrete strength is considerably higher as a result of on-going cement hydration during many years.

2.2 *Prototype of the bridge*

In order to simulate an actual bridge as closely as possible, a 1:2 scale was used to design the proto-type. Fig. 2 shows the prototype in the laboratory. To consider the most unfavourable effects in the investigation, the following lower bounds were considered during design.

1. In a typical real bridge, the interface between the side of the upper flange of the girder and the cast in-situ deck is inclined to 5 degrees at one side of the deck slab but the prototype was provided with inclined interfaces at both sides.
2. The spacing of the transverse prestressing was derived from the general spacing of 800 mm c/c in the actual bridge to 400 mm c/c in the model.
3. Most of the tests were done with a load applied in-between two adjacent transverse prestressing ducts in the deck. This gives a lower bound for the bearing capacity as compared to the capacity when testing directly above a prestressing duct.
4. Three transverse prestressing levels were applied: 0.5, 1.25 MPa and 2.5 MPa. Although the usual TPL in a real bridge is 2.5 MPa, the value of 1.25 was applied to regard the eventual effect of tendon failure. A TPL of 0.5 MPa simulated the control specimen. To adjust the prestressing level unbonded prestressed bars were applied.



Figure 2. Test-setup in the laboratory

2.3 Components of the test-setup

The deck prototype was 12 m long (the span length was not scaled down and therefore no diaphragms were required for 12 m length) and 6.4 m wide consisting of four precast concrete girders placed at 1800 mm c/c distance (Fig. 3). The exterior girders had an extended width of 125 mm at the exterior flanges to make sure that the prestressing and the confining effect was introduced adequately. The cross section of the girders is as shown in Fig. 4. Some of the interfaces between the deck slab panel and the girder flange were skew (1:20) and their location in plan is shown in Fig. 3b. The deck slab was cast *in situ* and post-tensioned in the transverse direction with a clear span of 1050 mm and had a thickness of 100 mm (Fig. 3c). Regular steel reinforcement was provided at both top and bottom with \varnothing 6 mm bars at 200 mm c/c in the longitudinal direction and \varnothing 6 mm bars at 250 mm c/c in the transverse direction. The transverse prestressing steel consisted of \varnothing 15 mm unbonded bars post-tensioned to the desired level. The interface between the slab and the girder was indented and had an inclination of 1:20.

The two transverse beams, 810×350 mm, were cast at 525 mm from each end of the bridge deck (Fig. 3a). The top of the transverse beams was at 190 mm from the top of the girders. The beams were reinforced with \varnothing 8 mm stirrups at 250 mm c/c, and ten \varnothing 12 mm bars in

four layers in the longitudinal direction. The prestressing consisted of \varnothing 15 mm bars in the transverse direction stressed to the same level as the deck slab. More details regarding the test setup can be found in Amir (2014).

2.4 Material properties

The concrete compressive strength was measured on cubes and converted to cylinder strength as per Model code 2010 (fib 2012) and the tensile strength was measured by splitting tensile strength test. For the deck slab and the transverse beams, the mean

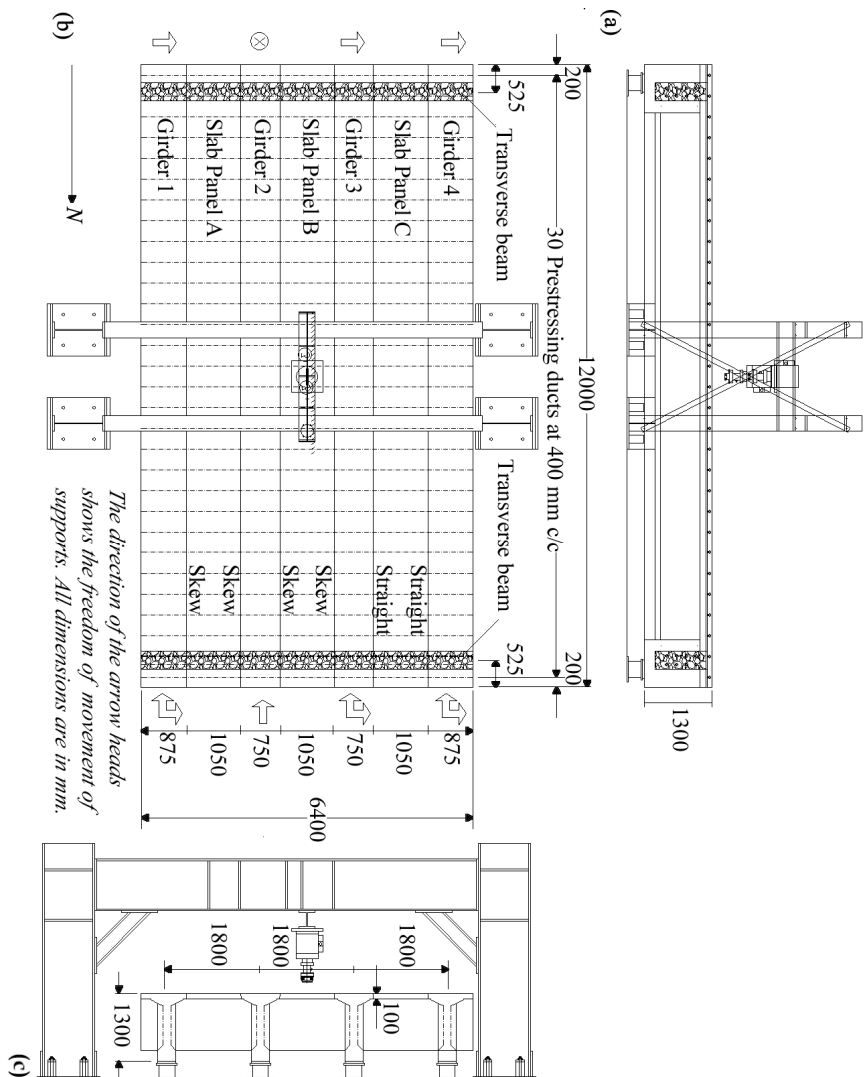


Figure 3. Test setup: a) Longitudinal side view b) Plan c) Transverse side view. All dimensions are in mm.

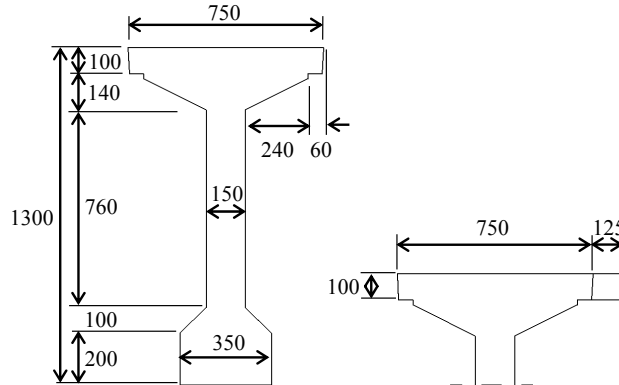


Figure 4. Cross section of prototype girder; on the left a typical interior girder and on the right an exterior girder with an extended flange width of 125 mm. All dimensions are in mm.

concrete compressive cylinder strength f_{cm} was 65 MPa, the mean splitting tensile strength f_{ctm} was 5.41 MPa and the modulus of elasticity, f_{cm} was calculated as 39 GPa. The characteristic tensile strength f_{pk} of the prestressing bars in the deck slab and transverse beams was 1100 MPa and the mean yield strength f_{sy} of the ordinary steel reinforcement was 525 MPa. For the girders, f_{cm} was 75 MPa, f_{ctm} was 6.30 MPa and the modulus of elasticity f_{cm} was calculated as 41 GPa.

2.5 Testing program

Nineteen static tests were performed by applying a concentrated load simulating a single or double wheel print load through a hydraulic actuator attached to an overhead reaction frame bolted to the floor (Fig. 5). The concentrated load was according to NEN-EN 1991-2:2003 (CEN 2003) Load Model 1 (Fig. 6). The wheel print of 400×400 mm was scaled down to 200×200 mm. The double load consisted of two point loads placed at a distance of 600 mm c/c, scaled down from 1200 mm c/c. Table 1 gives the test configuration and sequence. Generally speaking, four types of test were performed.

1. Single point load acting at mid span of deck slab panel, P1M.
2. Single point load acting close to the girder flange-deck slab interface/joint, P1J.
3. Double point loads at 600 mm c/c acting at mid span of deck slab panel, P2M.
4. Double point loads at 600 mm c/c acting close to the girder flange-deck slab interface/joint, P2J.

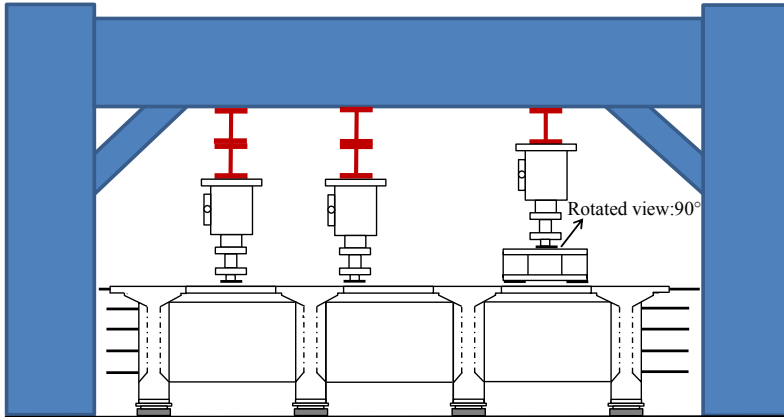


Figure 5. Single and double loads (not drawn to scale)

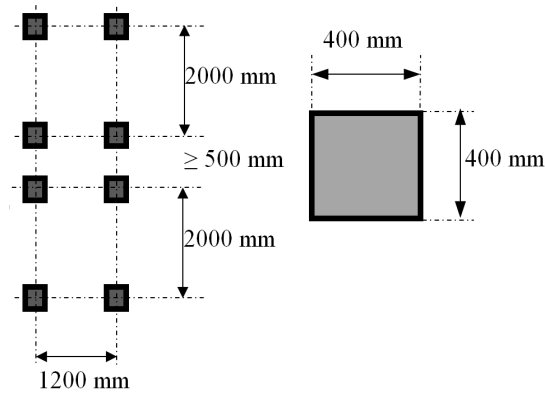


Figure 6. Eurocode load configuration and wheel print (Load model 1, NEN-EN 1991-2:2003).

Both exterior (A and C) and interior (B) deck slab panels were tested at various positions along the length of the deck. In almost all the interface (J) tests, the load was applied at 200 mm from the interface (c/c), except for Test BB3 & 4 with a TPL of 2.5 MPa where the center of the loading plate was at 110 mm from the interface. Tests were mostly performed by placing the center of the loading plate in-between the transverse prestressing ducts (BD), however, a few tests were carried out with the load just above a duct (AD). The size of the loading plate was 200×200 mm in all the tests except in test BB19 where a Eurocode Super single wheel tire C, i.e. a rectangular wheel print of 115×150 mm size (1:2 scale) was used. The transverse prestressing levels (TPLs) used were 0.5 MPa, 1.25 MPa and 2.5 MPa.

The test positions are shown in the deck slab plan in Figure 7 and the numbers are marked according to the sequence of the tests performed. The punching shear capacity obtained from the experiments is given in Table 2. Detailed test reports can be found in Stevin Report No. 25.5.13-06 (Amir & van der Veen 2013).

3 Numerical analysis

A 3D solid finite element model of the prototype bridge deck (Fig. 8a and 8b) was developed in the FEA software package TNO DIANA 9.4.4 conforming to recommendations of RTD 1016:2012 (2012). The model consisted of 3D solid elements

Table 1. Testing configuration and sequence

#	Test	Panel	Offset{1} mm	Load type	TPL MPa	Joint	Designation
1	BB1	C-Midspan	800	Single (BD)	2.5	Straight	C-P1M-ST
2	BB2	A-Midspan	800	Single (BD)	2.5	Skewed	A-P1M-SK
3	BB3	A-Interface	2400	Single (BD)	2.5	Skewed	A-P1J-SK
4	BB4	C-Interface	2400	Single (BD)	2.5	Straight	C-P1J-ST
5	BB5	C-Midspan	3100	Double (BD)	2.5	Straight	C-P2M-ST
6	BB6	A-Interface	3100	Double (BD)	2.5	Skewed	A-P2J-SK
7	BB7	C-Midspan	5400	Single (BD)	2.5	Straight	C-P1M-ST
8	BB8	C-Midspan	11200	Single (BD)	1.25	Straight	C-P1M-ST
9	BB9	A-Midspan	11200	Single (BD)	1.25	Skewed	A-P1M-SK
10	BB10	A-Interface	9600	Single (BD)	1.25	Skewed	A-P1J-SK
11	BB11	C-Midspan	9600	Double (BD)	1.25	Straight	C-P2M-ST
12	BB12	A-Interface	8200	Double (BD)	1.25	Skewed	A-P2J-SK
13	BB13	C-Midspan	8200	Single (AD)	1.25	Straight	C-P1M-ST
14	BB14	C-Interface	6600	Single (AD)	1.25	Straight	A-P1J-ST
15	BB15	A-Midspan	6600	Single (AD)	1.25	Skewed	A-P1M-SK
16	BB16	B-Midspan	6600	Double (BD)	2.5	Skewed	B-P2M-SK
17	BB19 {2}	B-Midspan	3600	Single (BD)	2.5	Skewed	B-P1M-SK
18	BB21	B-Midspan	800	Single (BD)	0.5	Skewed	B-P1M-SK
19	BB22	B-Midspan	5000	Single (BD)	0.5	Skewed	B-P1M-SK

{1} From North end of the deck

{2} Test performed on 1:2 scale Eurocode Super single wheel tire C (115×150 mm)

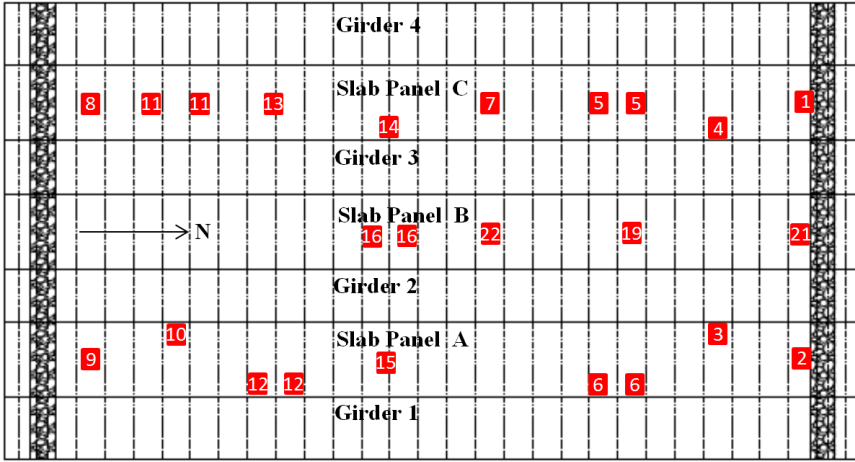


Figure 7. Deck slab test positions (BB1-BB22). Duct positions are also labelled.

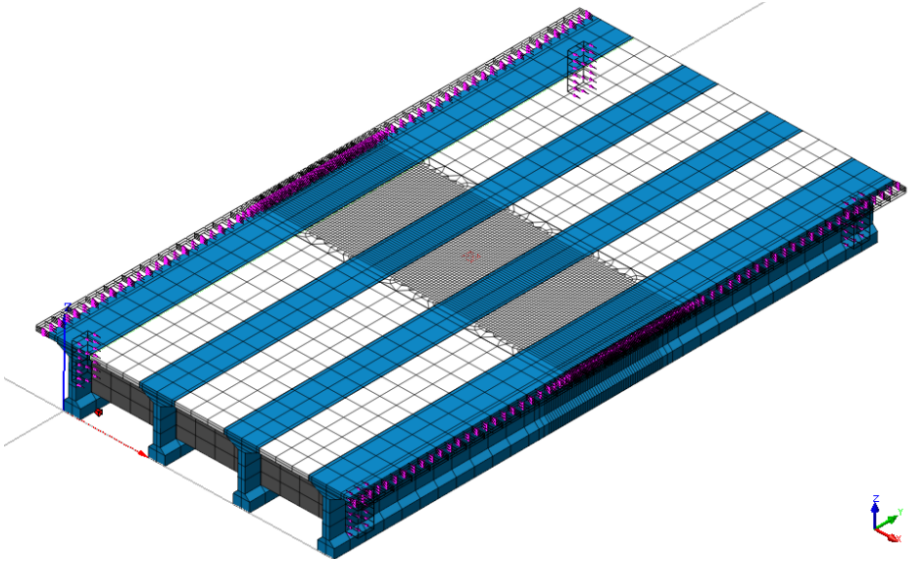


Figure 8a. 3D solid finite element bridge model

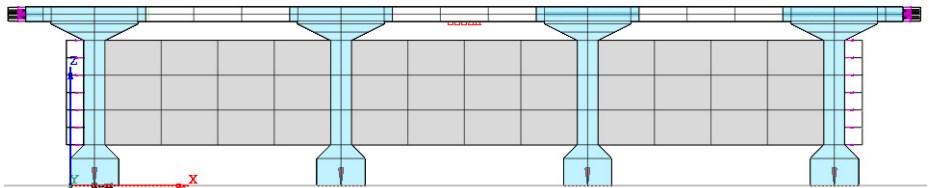


Figure 8b. The transverse cross-section of the 3D solid, finite element bridge model

(CHX60 and CTP45) with a fine mesh around the loading area and a course mesh away from the loading to reduce the time for computation. A layer of composed elements (CQ8CM) was provided in the fine mesh area to calculate compressive membrane forces (in-plane force N_{xx}). Ducts at 400 mm c/c were provided only in the fine mesh area around the loading position. Prestressing pressure was applied according to the required level of transverse prestressing in the deck slab and the transverse beams. An embedded reinforcement grid based on the actual steel reinforcement ratio was provided in the deck slab panels at the top and bottom in the horizontal direction as well as the vertical direction. A displacement controlled load was applied over an area of 200×200 mm simulating the wheel print impression on the deck slab with the exception of BB19 with a load area of 115×150 mm.

3.1 *Material models and additional nonlinear material properties*

For the material properties of the girders and transverse beams that were analyzed as linear, reference is made to section 2.4. For the nonlinear analysis of the deck slab, a smeared cracking “Total strain crack rotating model” was selected. An elastic-perfectly plastic model, CONSTA, was used for the concrete behavior in compression, whereas, an exponential softening curve, HORDIJK (Hordijk 1991), was used for the concrete behavior in tension. A fracture energy G_f of 0.15 N/mm was assumed for the deck slab concrete (for a maximum aggregate size of 20 mm, MC90 gives a value of 0.135 N/mm for the fracture energy, whereas MC2010 gives a value of 0.21 N/mm). Poisson’s ratio ν , for all the concrete components, was taken as 0.2. For the embedded grid reinforcement, the von Mises plasticity criterion was used with a Poisson ratio of 0.3.

3.2 *Iteration method and convergence criteria*

Both physical and geometrical nonlinearities were applied to the system. Composed elements were generated while giving the analysis commands. An incremental-iterative procedure was used for the nonlinear analysis and the modified Newton Raphson method was used for the solution. The prestressing load was applied to the bridge deck in a single step. After that a displacement-controlled load was applied with a step size of 0.1 mm unless the solution diverged, in which case the displacement increment was reduced to 0.05 mm. Since the applied load was displacement-controlled, the default force and energy based convergence criterion was employed.

3.3 *Types of the numerical analyses*

All the experiments were simulated as closely as possible using the 3D FE model. For most cases the deck slab was analyzed non-linearly while the girders and the transverse beams remained in the linear range. The only exceptions to this were the tests BB3 & 4. The flange of the adjoining girder was analyzed as nonlinear since the load was too close to the interface (110 mm c/c) and linearity of the flange would have induced a much higher capacity than in reality. The in-plane normal force (N_{xx} from composed elements) of each simulation, found from the nonlinear analyses of the 3D solid, finite element model bridge, will later be used to incorporate CMA in Model Code 2010 punching shear provisions (section 7.2).

4 **Comparison of experimental and numerical results**

The ultimate punching loads from the experiments P_T and finite element analysis P_{FEA} are summarized and compared in Table 2. The average ratio of P_T/P_{FEA} is 1, the standard deviation is 0.10 and the coefficient of variation is 10%. Both the experimental and numerical results showed that an increase in the TPL increased the punching shear capacity when loads were applied at midspan or at the interface.

Generally, for single load tests, the finite element approach gave conservative results, while for double loads, the bearing capacities were over-estimated but within reasonable limits as compared to the experimental results. The only exception was test BB12 where the finite element simulation result gave an error of 21% as compared to the experimental result but this test had failed at an unexpected lower load.

5 **Theoretical analysis**

5.1 *Comparison of predictions and experimental results*

The punching shear capacity of single load tests with failure in brittle punching is calculated according to the background report 25.5-02-37-prENV 1992-1-1:2002 (2002) and ACI 318-11 (2011). The TPLs investigated are 0.5, 1.25 and 2.5 MPa. The mean material properties used are described in section 2.4. No material factors have been used.

The background report 25.5-02-37-prENV 1992-1-1:2002, section 6.4, calculates the design punching shear capacity as

$$V_{r,EC2} = v_{Rd,c} u d \quad (N, mm) \quad (1)$$

where, $v_{Rd,c} = C_{Rd,c} k \sqrt[3]{100 \rho_l f_{cm}} + k_1 \sigma_{cp}$ (N, mm), $C_{Rd,c} = 0.18/\gamma_c$, ($\gamma_c = 1$ as no material factors are used) and $k_1 = 0.08$. On the basis of the background report, for further calculations, it is assumed that an average prediction is obtained by replacing $C_{Rd,c}$ in Eq. 1 by 0.18. The remaining parameters remain the same as in NEN-EN 1992-1-1:2005. The ACI 318-11 punching shear equation is

Table 2. Comparison of experimental and numerical results

Test BB.	TPL MPa	Designation	P_T kN	P_{FEA} kN	P_T/P_{FEA}
1.	2.5	C-P1M	348.7	302.3	1.15
2.	2.5	A-P1M	321.4	302.3	1.06
3.	2.5	A-P1J	441.6	429.9	1.03
4.	2.5	C-P1J	472.3	429.9	1.10
5.	2.5	C-P2M	490.4	529.9	0.93
6.	2.5	A-P2J	576.8	537.0	1.07
7.	2.5	C-P1M	345.9	302.3	1.14
8.	1.25	C-P1M	284.5	271.4	1.05
9.	1.25	A-P1M	258.2	271.4	0.95
10.	1.25	A-P1J	340.3	300.7	1.13
11.	1.25	C-P2M	377.9	453.4	0.83
12.	1.25	A-P2J	373.7	454.9	0.82
13.	1.25	C-P1M (AD)	322.9	363.1	0.89
14.	1.25	A-P1M (AD)	295.9	294.0	1.01
15.	1.25	A-P1M (AD)	359.7	363.1	0.99
16.	2.5	B-P2M	553.4	592.7	0.93
19.	2.5	B-P1M (SLP)	317.8	306.0	1.04
21.	0.5	A-P1M	243.8	274.6	0.89
22.	0.5	A-P1M	257.5	274.6	0.94
			Mean		1.00
			Standard deviation		0.10
			Coefficient of variation (COV)		0.10

Notations: AD = Above the duct, BD = In-between the ducts, SLP = Small loading plate (115×150 mm), P_T = Test ultimate load and P_{FEA} = Finite element analysis (FEA) ultimate load.

$$V_{r,ACI} = (0.29\sqrt{f_{cm}} + 0.3\sigma_{cp})b_0d \quad (N, mm) \quad (2)$$

where, $0.9 \text{ MPa} \leq \sigma_{cp} \leq 3.5 \text{ MPa}$ (σ_{cp} is the average prestressing in each direction) and $f_{cm} < 35 \text{ MPa}$. The limitation on σ_{cp} has been ignored here. Calculations are done for both $f_{cm} = 35 \text{ MPa}$ and 65 MPa . The remaining parameters are as defined in ACI 318-11 (2011).

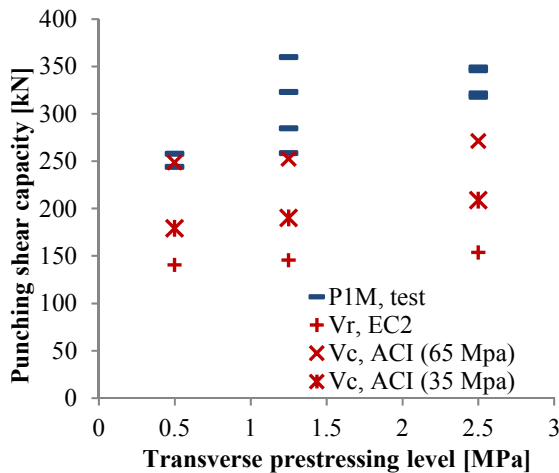


Figure 9. Comparison of experimental punching shear capacity of a single load at midspan (P1M, test) with that of background report 25.5-02-37-prENV 1992-1-1:2002 ($V_{r,EC2}$) and ACI 318 ($V_{r,ACI}$)

Figure 9 shows that the basic equations used for both codes underestimate the punching shear capacity of laterally restrained prestressed slabs. This lack of capacity is attributed to the ignorance of CMA that is present in such slabs. However, it can be observed that the capacity prediction for ACI 318, $V_{r,ACI}$ (65 MPa), when the limit on f_{cm} is not followed is better, although still conservative for higher TPLs. For 0.5 MPa, it is comparable with the test results. Results from the background report 25.5-02-37-prENV 1992-1-1 ($V_{r,EC2}$) are conservative even for a very low level of 0.5 MPa TPL. It is obvious that the contribution of prestressing (σ_{cp}) is low in both ACI 318 and the background report EC2. It is clear that currently no code is fully suitable for the prediction of the punching shear capacity of prestressed slabs considering compressive membrane action and there is a dire need to develop a method for such cases.

5.2 Model Code 2010 punching shear provisions: The Critical Shear Crack Theory

In this section, the Critical Shear Crack Theory, CSCT, (Muttoni 2008, Clément et al. 2013) is applied on the transversely prestressed bridge deck under study using the Levels of Approximation (LoA) approach (Muttoni and Fernández Ruiz 2012a, 2012b) with some modifications. Provisions from the Model Code 2010 (*fib* 2012) regarding punching shear in slabs using CSCT are used in combination with numerically found in-plane forces comprising compressive membrane action.

According to the CSCT, the width w of the critical shear crack can be correlated to the product of the rotation ψ and the flexural effective depth d of the slab ($w \propto \psi d$), see Figure 10.

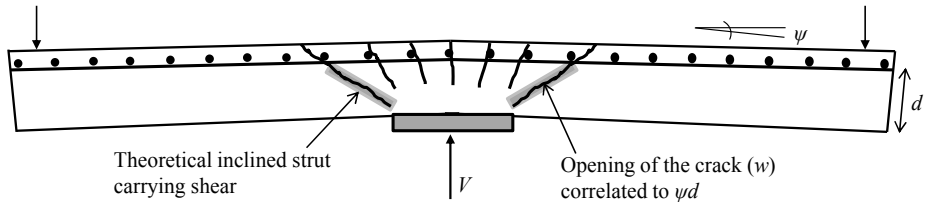


Figure 10. The Critical Shear Crack Theory, CSCT (Muttoni 2008)

Two equations are solved iteratively:

1. The failure criterion representing the available punching shear strength.
2. The load-rotation relationship representing the shear force for a given rotation.

A higher level of approximation requires a more precise calculation. The intersection point of the two curves gives the punching load and is influenced by the presence and type of an in-plane force (for case of prestressed slabs) as shown in Figure 11.

Equation 3 gives the failure criterion of the Critical Shear Crack Theory. This equation does not involve any material factors and is based on mean strengths.

$$\frac{V_R}{b_0 d_v \sqrt{f_{cm}}} = \frac{\frac{3}{4}}{1 + 15 \frac{\psi d}{d_{g0} + d_g}} \quad (3)$$

where, V_R is the shear strength, b_0 is the length of the control perimeter at $d_v/2$ of the edge of the supported area, d_v is the shear-resisting effective depth of the member, f_{cm} is the mean compressive strength of the concrete, ψ is the rotation and is calculated depending

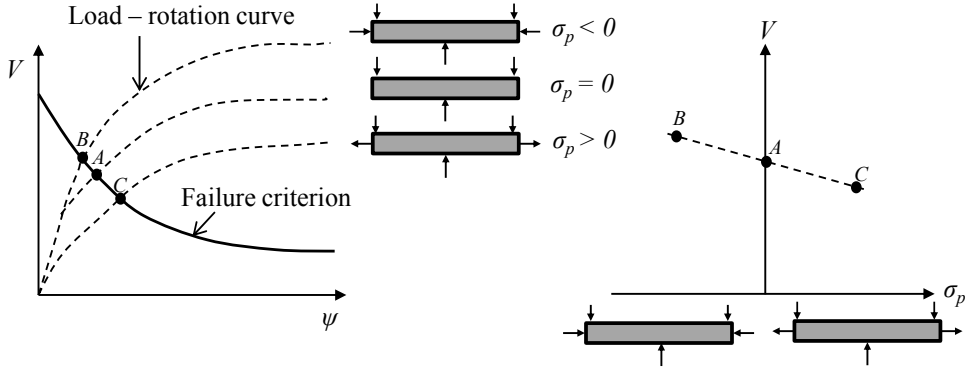


Figure 11. The Critical Shear Crack Theory: Influence of an in-plane force σ_p on the punching shear capacity V (Clément et al. 2013)

on the required LoA, d is the flexural effective depth of the member, d_{g0} is the maximum aggregate size and d_g is the reference aggregate size equal to 16 mm.

The rotation at failure ψ (in Eq. 3) can be evaluated by using the Levels-of-Approximation (LoA) approach. In the Model Code 2010, the influence of prestressing (Fig. 11) on punching shear strength is explored at the LoA II and III (typical LoA to be used for structures where punching shear strength is governing). No calculations are made at LoA I for prestressed slabs. In LoA IV, the rotation ψ can be calculated on the basis of a nonlinear flexural analysis of the structure and accounting for cracking, tension-stiffening effects, yielding of the reinforcement and any other nonlinear effect relevant for providing an accurate assessment of the structural bearing capacity (fib 2012). Instead of using this traditional LoA approach, a modified LoA approach was introduced in Amir (2014) to calculate the capacity of the model bridge deck and is employed here. The following general equation will be used to calculate the rotations.

$$\psi = 1.5 \frac{r_s}{d} \frac{f_{sy}}{E_s} \left(\frac{m_s - m_p}{m_R - m_p} \right)^{1.5} \quad (4)$$

In Equation 4, $m_s \approx V/8$, for inner columns without unbalanced moments (Muttoni 2008, Clément et al. 2013), $m_R = \rho f_{sy} d^2 (1 - 0.5 \rho f_{sy} / f_{cm})$ and $m_p = n(h/2 - d/3 + e)$. Here, V is the acting shear force, ρ is the steel reinforcement ratio, f_{sy} is the yield strength of the steel, f_{cm} is the mean compressive cylinder strength of concrete, n is the normal force per unit length, h is the depth of the slab, d is the effective depth and e is the eccentricity of the

normal force from the center of gravity of the section. As a sign convention, the decompression moment is considered positive when it leads to compressive stresses on the top side of the slab (Clément et al. 2013). For the current case, no eccentricity exists since the prestressing bars are applied at mid-depth. ρ_{ps} (geometric prestressing steel ratio) and f_{pe} (effective prestress) representing an equivalent steel will be used in place of ρ and f_{sy} , respectively, to determine the flexural strength of the deck slab panel with unbonded transversely prestressed bars. Similar to the verification procedure, the flexural effective depth of the section will be taken equal to the shear resisting effective depth in the assessment calculations ($d = d_v = 87$ mm). In the Elementary Level of Approximation, the load-rotation relationship is established using the transverse prestressing force as the normal force n . This serves as a lower bound for the ultimate capacity (Fig. 12).

In the Advanced Level of Approximation, the load-rotation relationship is established using the overall in-plane force (sum of transverse prestressing force and compressive membrane force) as the normal force n , found from the nonlinear analyses of the 3D solid, finite element model bridge described in Section 5 (N_{xx} from composed elements). This serves as the upper bound of the ultimate capacity. In this way, compressive membrane

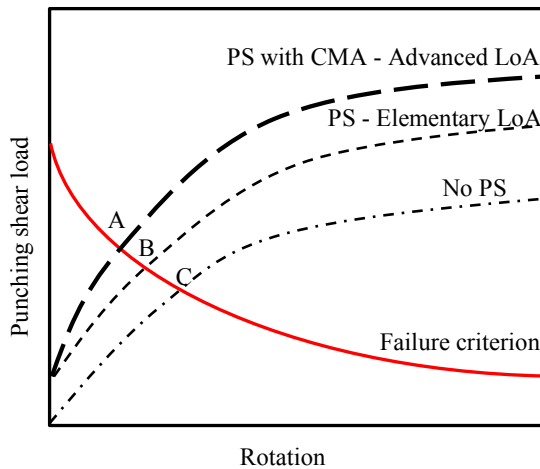


Figure 12. The Level of Approximation (LoA) approach for the analysis of the transversely prestressed deck slab (PS = Prestressing, CMA = Compressive membrane action). The elementary LoA giving punching shear load B and the advanced LoA giving punching shear load A. For no prestressing, the failure load is C.

action is automatically incorporated in the load-rotation relationship (Fig. 12). Detailed calculations of all experimental cases using the critical shear crack theory and the modified Level of Approximation approach can be found in Amir (2014). Results (P_{CSA}) can be found in Table 3. It can be observed that the transverse prestressing level affects the bearing (punching shear) capacity positively.

6 Safety analysis of the model bridge deck

In this section, the experimental, numerical and theoretical (CSCT) results are compared with the Eurocode Load Model 1 design wheel load to assess if the structure is able to carry the modern traffic loads. Results with 0.5 MPa have not been considered since they were performed only as control cases and such a low level of TPL does not exist in the type of the bridge under study. Analyses with wheel print above the ducts have also been disregarded although they give a higher capacity.

6.1 The Global Safety format and model uncertainty

Cervenka (2013) compares in detail various methods of global safety assessment found in the MC2010; the Global Resistance Factor Method (GRF), full probabilistic analysis, Estimation of Coefficient of Variation of Resistance Method (ECOV) and Partial Safety Factors (PSFs). Generally, the global resistance factor (GRF) is considered the most promising format to be used for concrete structures since it is easy to use with an adequate safety margin. The nonlinear analysis is performed using mean values for the material characteristics and geometrical properties. The ultimate limit state verification requires a comparison of design resistance and design loads expected on the structure. The design equation is:

$$F_d < R_d \quad (5)$$

where, F_d is the design action and R_d is the design resistance. Both the action and resistance have individual safety margins incorporated into them (Cervenka 2013). The safety margin for the resistance part can be expressed as:

$$R_d = \frac{R_m}{\gamma_{GL}} \quad (6)$$

The calculated resistance R_m , using mean values for the material strengths, is divided by a global resistance factor γ_{GL} to obtain the design value for the structural resistance R_d . The

guidelines for the nonlinear finite element analysis of concrete structures (RTD 1016 2012) give $\gamma_{GL} = 1.2 \times 1.06 = 1.27$, where γ_{GL} is the product of the safety and the model coefficients. However, the mean resistance in the Model Code 2010 (fib 2012) and in RTD 1016 (2012) is based on fictitious values ($f_{cm} \approx 0.85 f_{ck}$) and not the actual mean strengths. In the present study, since the actual mean strengths are used, therefore, γ_{GL} is further divided by 0.85 to obtain a factor of 1.5 ($\gamma_{GL}' = 1.27/0.85 = 1.5$). The design load F_d is obtained by multiplying the characteristic load with a partial factor γ_Q . The characteristic wheel load, Q_K according to the Load Model 1 of EC2¹ is 150 kN for a single wheel (300 kN for a double load) and 300 kN for an axle. Hence the actions part of the Eq. 5 can be rewritten as

$$F_d = \gamma_Q Q_K \quad (7)$$

The Ministry of Infrastructure and the Environment in the Netherlands, Rijkswaterstaat, allows a partial factor for traffic actions γ_Q of 1.25 for existing bridges built before 2012 in RBK Table 2.1 (RTD 1006 2013) but a partial factor of 1.5 according to NEN-EN1990+A1+A1/C2:2011/NB:2011 (Table NB.13-A2.4(B), CC3) for new bridges is used here conservatively.

6.2 Factor of safety (FOS) of the model bridge deck

In this section, a factor of safety of the model bridge deck against traffic loads is calculated. The resistance R_m is taken equal to the ultimate (punching) loads from the tests, the finite element results and the critical shear crack theory results at an advanced LoA (P_T , P_{FEA} and P_{CSA} respectively) from the analyses of the 1:2 scaled bridge model. The test design resistance $R_{md,T}$ is calculated by applying Level II method² on the test ultimate load P_T (the resistance factor for test results, $\gamma_T = \mu_{RD}/B_{RD} = 1.5$). The FEA design resistance $R_{md,FEA}$ is obtained by dividing P_{FEA} by γ_{GL}' (1.5). Design resistance using CSCT³ $R_{md,CSA}$ is calculated for the model bridge deck at an advanced LoA with the appropriate material and safety factors. The scaled down design wheel load F_{md} is obtained by multiplying the characteristic load Q_K with a partial factor γ_Q (1.5) and dividing by the force scale factor ($x^2 = 2^2$). An average factor of safety of 3.71 is obtained by dividing the

¹ The ultimate distributed load is not taken into account. Also, the Load Model 2 of EC2 is not being considered, as the wheel footprint of only Load Model 1 was used in all the analyses.

² $B_{RD} = \mu_{RD}(1 - \alpha_{BR}\beta\delta_{BR})$, where $\alpha_{BR} = 0.8$, $\beta = 3.8$ and $\delta_{BR} = 0.11$ Amir (2014). Therefore, $\gamma_T = \mu_{RD}/B_{RD} = 1.5$.

³ Refer to the approach described in section 7.2.

design loads with the design resistance using the experimental, numerical and theoretical (CSCT) analysis results (Table 3).

7 Conclusions

The following important conclusions can be drawn:

1. An increase in the TPL linearly increases the punching shear capacity when loads are applied at midspan or at the interface.
2. Punching shear failures can be well predicted with nonlinear finite element analysis of 3D solid models. The use of composed elements can lead to the determination of in-plane forces as well as the level of compressive membrane

Table 3. Calculation of FOS for the model bridge deck using the actual analyses results

BB	TPL	P_T	P_{FEA}	P_{CSA}	$R_{md,T}$	$R_{md,FEA}$	$R_{md,CSA}$	Test	FEA	CSCT
								FOS	FOS	FOS
								$\frac{R_{md,T}}{F_{md}}$	$\frac{R_{md,FEA}}{F_{md}}$	$\frac{R_{md,CSA}}{F_{md}}$
		MPa	kN	kN	kN	kN	kN			
					$\frac{P_T}{\gamma_T}$	$\frac{P_{FEA}}{\gamma_{GL'}}$				
1	2.50	348.7	302.3	311	232	202	234	4.13	3.58	4.16
2	2.50	321.4	302.3	311	214	202	234	3.81	3.58	4.16
3	2.50	441.6	429.9	422.4	294	287	325	5.23	5.10	5.78
4	2.50	472.3	429.9	422.4	315	287	325	5.60	5.10	5.78
5	2.50	490.4	529.9	453.3	327	353	346	2.91	3.14	3.08
6	2.50	576.8	537.0	482.3	385	358	346	3.42	3.18	3.08
7	2.50	345.9	302.3	311	231	202	234	4.10	3.58	4.16
8	1.25	284.5	271.4	295.7	190	181	222	3.37	3.22	3.95
9	1.25	258.2	271.4	295.7	172	181	222	3.06	3.22	3.95
10	1.25	340.3	300.7	310.9	227	200	234	4.03	3.56	4.16
11	1.25	377.9	453.4	431.3	252	302	329	2.24	2.69	2.92
12	1.25	373.7	454.9	432.1	249	303	329	2.21	2.70	2.92
16	2.50	553.4	592.7	482.3	369	395	369	3.28	3.51	3.28
19	2.50	317.8	306.0	281.9	212	204	208	3.77	3.63	3.70
Factor of safety								3.65	3.56	3.93
Average factor of safety									3.71	

action in a laterally restrained slab which were previously difficult to determine using analytical techniques.

1. Currently no design codes make use of the beneficial effects of compressive membrane action. Eurocode 2 and ACI 318 give conservative results since they consider a very low contribution of the in-plane forces.
2. The theoretical analysis results using CSCT with an advanced LoA prove the effectiveness of considering compressive membrane action in the load-rotation behavior of a structure.
3. For the model bridge, an average factor of safety of about 3.71 is obtained against the design wheel load. Such a high safety margin is due to the beneficial effect of compressive membrane action that gives a reserve capacity for old bridges.

Acknowledgements

The authors would like to express their appreciation for Rijkswaterstaat, Ministry of Infrastructure and the Environment, the Netherlands, for supporting this research.

References

- ACI Committee 318 (2011), Building Code Requirements for Structural Concrete (ACI 318-11) and Commentary (ACI 318R-11), American Concrete Institute, Farmington Hills, Michigan, USA.
- Amir, S. (2014), *Compressive membrane action in prestressed concrete deck slabs*, PhD thesis, Delft University of Technology, Delft, the Netherlands, pp 282.
- Amir, S., van der Veen, C., Walraven, J. C. & de Boer, A. (2014a), Bearing capacity of prestressed concrete deck slabs, Proceedings of the *fib congress 2014*, Mumbai, India.
- Amir, S., van der Veen, C., Walraven, J. C. & de Boer, A. (2014b), Numerical investigation of the bearing capacity of transversely prestressed concrete deck slabs, Proceedings of the *EURO-C 2014*, Computational Modelling of Concrete and Concrete Structures, St. Anton am Arlberg, Austria, pp. 999-1009.
- Background report 25.5-02-37 – prENV 1992-1-1:2002, Section 6.4 (2002), J. C. Walraven, Delft University of Technology, the Netherlands.
- Batchelor, B. de V (1990), Membrane Enhancement in Top Slabs of Concrete Bridges, Concrete Bridge Engineering, Performance and advances, pp. 189-213.
- CAN/CSA-S6-06 (2006), Canadian Standard Association: Canadian Highway Bridge Design Code (CHBDC), Canada.

- CEN (2003), Eurocode 1 – Actions on Structures - Part 2: Traffic loads on bridges, NEN-EN 1991-2, Comité Européen de Normalisation, Brussels, Belgium, 168 pp.
- CEN (2005), Eurocode 2 – Design of Concrete Structures - Part 1-1: General Rules and Rules for Buildings, NEN-EN 1992-1-1, Comité Européen de Normalisation, Brussels, Belgium, 229 pp.
- Cervenka, C. (2013), Reliability-based non-linear analysis according to fib Model Code 2010, *Structural Concrete*, Volume 14, No. 1, pp. 19-28
- Clément, T., Ramos, A. P., Fernández Ruiz, M. & Muttoni, A. (2013), Design for punching of prestressed concrete slabs, *Structural Concrete*, Volume 14, pp. 157-167.
- fib (2012), Model Code 2010-Final Draft Volume I and II, fib Bulletin 65 and 66.
- Hon, A., Taplin, G. & Al-Mahaidi, R. S. (2005), Strength of reinforced concrete bridge decks under compressive membrane action, *ACI Struct. Journal*, Vol. 102, No. 3, pp. 393-401
- Hordijk, D. A. (1991), *Local Approach to Fatigue of Concrete*, PhD thesis, Delft University of Technology, the Netherlands, 210 pp.
- Muttoni, A. (2008), Punching shear strength of reinforced concrete slabs without transverse reinforcement, *ACI Structural Journal*, Volume 105, No. 4, pp. 440-450.
- Muttoni, A. & Fernández Ruiz, M. (2012a), The levels-of-approximation approach in MC 2010: application to punching shear provisions, *Structural Concrete*, Vol. 13, pp. 32-41.
- Muttoni, A. & Fernández Ruiz, M. (2012b), Levels-of-Approximation Approach in Codes of Practice, *Structural Engineering International*, Volume 22, No. 2, pp. 190-194.
- NEN 6720:1995, Regulations for concrete: structural requirements and calculation methods (in Dutch), Dutch Normalisation Institute (NEN).
- NEN-EN 1990+A1+A1/C2:2011/NB: 2011, National Annex to NEN-EN 1990+A1+A1/C2: Eurocode: Basis of structural design, 37 pp.
- RTD 1016 (2012), Guidelines for nonlinear finite element analysis of concrete structures, Rijkswaterstaat Technisch Document (RTD) 1016:2012.
- RTD 1006 (2013), RBK, Richtlijnen Beoordeling Kunstwerken, Rijkswaterstaat Technisch Document (RTD) 1006:2013.
- Stevin Report No. 25.5.13-06, Amir, S. & van der Veen, C. (2013), Bearing capacity of transversely prestressed concrete decks, Delft University of Technology, The Netherlands, 243 pp.
- Transit New Zealand Ararau Aotearoa (2003): New Zealand Bridge Manual, 2nd Edition.
- UK Highways Agency, BD 81/02 (2002): Use of Compressive Membrane Action in bridge decks, *Design Manual for Roads and Bridges*, Vol. 3, Section 4, part 20, 20 pp.